

Effect of surface state hybridization on current-induced spin-orbit torque in thin topological insulator films

Cong Son Ho,^{1,*} Yi Wang,¹ Zhuo Bin Siu,¹ Hyunsoo Yang,¹ Seng Ghee Tan,² and Mansoor B. A. Jalil^{1,†}

¹*Department of Electrical and Computer Engineering,*

National University of Singapore, 4 Engineering Drive 3, Singapore 117576.

²*Data Storage Institute, Agency for Science, Technology and Research (A*STAR), 2 Fusionopolis Way, 08-01 Innova, Singapore*

(Dated: December 6, 2016)

We investigate the current-induced spin-orbit torque in thin topological insulator (TI) films in the presence of hybridization between the top and bottom surface states. We formulate the relation between spin torque and TI thickness, from which we derived the optimal value of the thickness to maximize the torque. We show numerically that in typical TI thin films made of Bi₂Se₃, the optimal thickness is about 3-5 nm.

PACS numbers: 72.25.Dc, 71.70.Ej, 71.10.Ca

I. INTRODUCTION

Spin torque is one of the most actively researched topics in spintronics. In spin-orbit coupling (SOC) systems, the resulting spin-orbit torque (SOT) comprises of two types: field-like torque [1–5] and damping-like torque [6, 7]. The SOT strength scales with the SOC strength, therefore one can obtain a large SOT signal in strong SOC systems, such as heavy metal/ferromagnet (Pt/Co) [8] and topological insulators (TI) [9–11].

Topological insulators possess strong SOC which translates to a large SOT effect. Moreover, the spin-locked topological surface states of TI are robust under effects of the time-reversal symmetric impurity scattering. These factors enable TI to be one of the most promising candidates for SOT devices. When a current is passed onto the TI surface (interface), a non-equilibrium spin density will be induced on that surface [9], which is directed in-plane and perpendicular to the applied current as a result of the spin-momentum locking of the surface states [9], similar to the Rashba-Edelstein effect [12]. Thus spin accumulation is proportional to the charge current flowing on the TI surface [1, 2, 9]. In addition, an out-of-plane spin density can be generated due to the Berry curvature of the spin texture in the momentum space [7, 13, 14], and due to the presence of the hexagonal-warping effect [15]. The two components, in-plane and out-of-plane spin density, are responsible for inducing an out-of-plane and in-plane torques, respectively.

In the study of current-induced SOT, spin torque efficiency (ratio of torque strength and current density in the TI - $\mathcal{T}/j_{\text{TI}}$, which is equivalent to spin Hall angle j_s/j_{TI}) is a crucial quantity. In 3D TI's, the surface state has a finite thickness and usually extends into the bulk material, up to 1 nm from the TI-vacuum interface [10, 16], and the current is supposed to flow entirely in the surface channel in ideal TI. However, in practical 3D TI's, the

bulk is not totally insulating [17], and thus the current in the TI can flow either in the surface and bulk channels. Since the bulk states do not exhibit any spin-momentum locking, TI with a large bulk conductance will induce a smaller torque on an adjacent ferromagnetic (FM) layer. Therefore, it is obvious that one has to reduce the TI thickness to reduce the relative contribution of the bulk [18–20], and enhance the torque efficiency. But how far can the thickness of a TI film be reduced?

Normally, a 3D TI film comprises of two surfaces (top and bottom surfaces, for example). In a typically thick TI film, the two surfaces are uncorrelated, i.e., the transport on one surface will not affect the other. However, if the film is made very thin, i.e., its thickness is comparable to the decay length of surface states, the two surface states become hybridized [21–24]. This hybridization is quantified by a tunneling coupling constant (Δ), which is thus a function of the TI thickness. Generally, Δ is larger as the thickness is reduced [21–23]. The effect of the surfaces hybridization on spin torque is as follows. When a charge current is passed onto the top surface in the x -direction, it can leak to the bottom surface through the tunneling effect [25]. While the current on the top surface induces a spin accumulation in the y -direction, its bottom counterpart induces a spin accumulation in the opposite, i.e., $-y$ -direction, since the two surface states have opposite helicities. As a result, the total spin accumulation is reduced with the hybridization effect. Thus, the spin torque is also reduced as the TI thickness is reduced. This dependence will be formulated subsequently in this paper.

From the above, we may surmise that the reduction in the TI thickness has two competing effects on the spin torque: (i) the torque strength is stronger as the bulk contribution is decreased; (ii) on the other hand, the torque strength becomes suppressed due to increasing hybridization of the surface states. Therefore, there is an optimal value of TI thickness which would maximize the torque efficiency.

Thus, the aim of this study is to investigate the spin torque in TI film in the presence of the hybridization ef-

* elehcs@nus.edu.sg

† elemhaj@nus.edu.sg

fect. We will formulate the relation between spin torque and TI thickness, from which we derive the optimal value of the thickness to maximize the torque. For the exemplary cases of Bi_2Se_3 or Bi_2Te_3 thin films, the optimal thickness is found to be about 3-5 nm. In previous experiments [9–11], the TI films have thickness in the range of 6-20 nm, which is far above the predicted optimal values. The paper is organized as follows: in Section II, we formulate the theory of spin torque in a topological insulator (TI) system coupled to a ferromagnetic (FM) layer. In Section III, we will apply the theory to the thin TI-FM film, where the hybridization between the top and bottom surface states is taken into consideration, and derive the optimal thickness for maximum torque efficiency. The conclusion is given in the last section.

II. THEORY

We will first formulate the spin-torque induced by charge current in a coupled FM/TI bilayer system in the absence of inter-surface hybridization. The Hamiltonian of the system is given by:

$$\mathcal{H} = \mathcal{H}_{\text{TI}} + J_{\text{ex}} \mathbf{m} \cdot \hat{\sigma}, \quad (1)$$

where the first term is the Dirac Hamiltonian of the topological surface state $\mathcal{H}_{\text{TI}} = \hbar v_F (\mathbf{k} \times \hat{z}) \cdot \hat{\sigma}$ with v_F being the Fermi velocity, $\hat{\sigma}$ is the vector the Pauli matrices. The last term is the s - d exchange interaction between itinerant electron and magnetization with J_{ex} being the exchange constant. We can rewrite Eq. (1) to express electron spin in an effective field as $\mathcal{H} = \mathbf{b} \cdot \hat{\sigma}$, where $\mathbf{b} = \hbar v_F (\mathbf{k} \times \hat{z}) + J_{\text{ex}} \mathbf{m}$. The eigenenergies are found as

$$\mathcal{E}_s(\mathbf{k}) = s \sqrt{(\hbar v_F k)^2 + (J_{\text{ex}})^2 + 2\hbar v_F J_{\text{ex}} \mathbf{m} \cdot (\mathbf{k} \times \hat{z})} \quad (2)$$

where $s = \pm 1$ which is for majority and minority electron, respectively, and we have used the fact that $|\mathbf{m}| = 1$. For a given value of momentum \mathbf{k} , Eq. (2) can be considered as the energy of the magnetic system. Thus, the torque field acting on the magnetization can be found by taking the functional derivative of $\mathcal{E}_s(\mathbf{k})$, *i.e.* [26],

$$\mathbf{H}^{\text{eff}} = -\frac{n}{\mu_0 M_s} \frac{\delta \mathcal{E}}{\delta \mathbf{m}}. \quad (3)$$

In the above, n is the charge density, and M_s is the saturated magnetization. Let us first consider the contribution from the lower band. In this case, from Eqs. (2) and (3), the torque field is

$$\mathbf{H}^{\text{eff}} = \frac{n \hbar v_F}{\mu_0 M_s} (\mathbf{k} \times \hat{z}). \quad (4)$$

The upper band will give rise to an opposite torque field. To obtain the above, we have assumed the strong exchange limit, *i.e.* $J_{\text{ex}} \gg \hbar v_F k_F$, $|b| \approx J_{\text{ex}}$, and the effective field is taken to the first order in $\hbar v_F k / J_{\text{ex}}$. The

net torque field is found by summing over all momentum space. In the absence of applied current, the expectation value of \mathbf{k} would vanish and so would the effective field. However, in the presence of some charge current \mathbf{j}_e^{ss} that flows on the surface, the average \mathbf{k} is finite and can be found as following. The charge current is expressed as $\mathbf{j}_e^{ss} = ne \langle \mathbf{v} \rangle$, where n is the sheet carrier density, and $\mathbf{v} = \frac{\partial H}{\hbar \partial \mathbf{k}} = v_F (\hat{z} \times \hat{\sigma})$ is the velocity. In the adiabatic limit, the electron spin is mostly aligned along the effective field as $\langle \hat{\sigma} \rangle = \mathbf{b}/|b|$, from which the charge current is $\mathbf{j}_e^{ss} = ne \frac{\hbar v_F^2}{J_{\text{ex}}} \langle \mathbf{k} \rangle + ne v_F (\hat{z} \times \mathbf{m})$. Rearranging the equation, we have

$$\langle \mathbf{k} \rangle = \frac{J_{\text{ex}}}{ne \hbar v_F^2} \mathbf{j}_e^{ss} - \frac{J_{\text{ex}}}{\hbar v_F} (\hat{z} \times \mathbf{m}). \quad (5)$$

Substituting Eq. (5) into Eq. (4), we obtain the current-induced torque field,

$$\mathbf{H}^{\text{eff}} = \eta_0 (\mathbf{j}_e^{ss} \times \hat{z}), \quad (6)$$

where $\eta_0 = \frac{J_{\text{ex}}}{ev_F \mu_0 M_s}$, and we have ignored the component that is parallel to \mathbf{m} , as this does not induce torque on the magnetization itself. The field in Eq. (6) is in-plane and it induces an out-of-plane torque on the magnetization as $\mathcal{T} = \mathbf{m} \times \mathbf{H}^{\text{eff}}$. Explicitly,

$$\mathcal{T} = \eta_0 \mathbf{m} \times (\mathbf{j}_e^{ss} \times \hat{z}). \quad (7)$$

In practice, an applied current j_e^0 in the system is composed of three different channels: (i) surface current j_e^{ss} , (ii) bulk current j_e^b , and (iii) shunting current through the FM layer j_e^{FM} , see Fig. 1. Therefore, out of the total applied charge current j_e^0 , only j_e^{ss} would generate a torque field and spin torque, following Eqs. (6) and (7). To obtain the relation between the surface current and the net current, we assume that the FM and TI layers have thicknesses t and d , and conductances G_{FM} and G_{TI} , respectively. The surface current is then given by

$$j_e^{ss}(d) = j_e^0 \frac{G_{\text{TI}}^{ss}}{G_{\text{TI}} + G_{\text{FM}}} = j_{\text{TI}} \frac{G_{\text{TI}}^{ss}}{G_{\text{TI}}}. \quad (8)$$

In the above, j_{TI} is the current flowing in the TI film, G_{TI}^{ss} is the conductance of TI surface, which is assumed to be unchanged as the thickness of the TI layer d is changed. Meanwhile, the total conductance of the TI layer G_{TI} increases with d [17], reflecting the increased contribution of the bulk channel. Therefore, the spin torque and torque field would generally be enhanced as d is reduced. In practice, TI films can be made very thin, *i.e.*, down to 2 nm [17], and therefore one may induce large spin torque in such systems. However, as the TI film thickness is reduced to below some critical value, the property of the surface state will be changed, *i.e.*, an energy gap is opened and the Dirac cone would disappear, as a result of the surface hybridization [16, 20, 22, 24]. As a consequence, all spin transport effects arising from the topological surface states will be modified accordingly. The effect of surface hybridization will be considered in the following section.

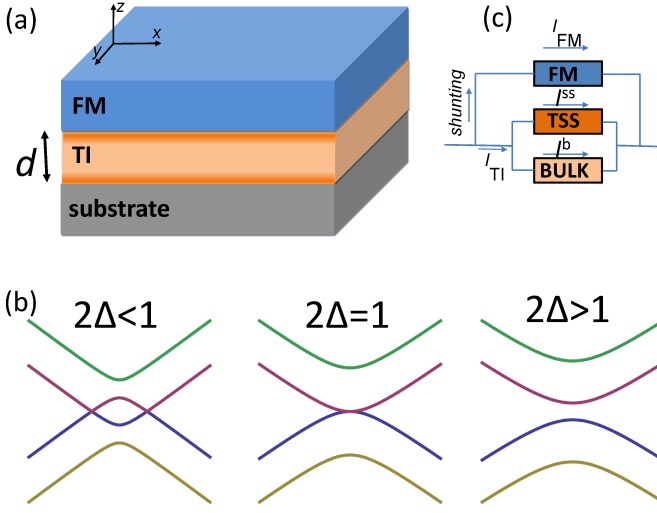


FIG. 1. (Color online) (a) Schematic diagram of bilayer ferromagnet/topological insulator. The TI film is of the thickness d . (b) Schematic energy \mathcal{E} versus k_x subbands near the Dirac points ($k_x = 0$) for various values of the tunneling element Δ . (c) Schematic diagram of the current distribution in the bilayer with I_{TI} being the current in the TI film, and I_{FM} being the shunting current through the FM layer. In the TI film, the current can flow in the surface state channel (I^{ss}) and bulk channel (I^b), respectively.

III. SPIN TORQUE WITH HYBRIDIZATION EFFECT

A. Effect of surface hybridization

In this Section, we will formulate the spin-orbit torque in a thin TI film with hybridization effect. In this case, both surface states (of top and bottom surfaces) are taken into account. We assume that the magnetic layer is only in contact with the top TI surface with the exchange coupling J_{ex} . The itinerant electron on the bottom surface may also couple to the FM, but with a weaker exchange coupling, which is then ignored for simplicity. In addition, we also disregard the asymmetry between the two interfaces, *i.e.*, FM/TI and TI/substrate interfaces.

The Hamiltonian of the system is then given by [24]

$$\mathcal{H} = \begin{bmatrix} \mathcal{H}_{TI} + J_{ex} \mathbf{m} \cdot \hat{\sigma} & \Delta I_2 \\ \Delta I_2 & -\mathcal{H}_{TI} \end{bmatrix}. \quad (9)$$

In the above, Δ represents the tunneling element (hybridization) between top and bottom surfaces, I_2 is the (2×2) unit matrix. The value of Δ has an inverse relation with the thickness of the TI film, *e.g.*, $\Delta = 0.05$ eV for $d = 5$ nm film, but increases to 0.25 eV for $d = 2$ nm [19]. In the range of small thickness, the tunneling element can be approximated as [21, 22]

$$\Delta \approx \frac{B_1 \pi^2}{d^2}, \quad (10)$$

where B_1 is a material-dependent parameter [20]. Note that the Fermi velocity is also thickness-dependent. However, the variation can be neglected as its values in the thick and thin film limits only differ by the order of 0.01 [22].

From the Hamiltonian in Eq. 9, the eigenenergies are given by

$$\mathcal{E}_{s\tau} = s\sqrt{U + \tau V}, \quad (11)$$

with $s, \tau = \pm 1$, and

$$U = \Delta^2 + \frac{J_{ex}^2}{2} + \hbar^2 v_F^2 \mathbf{k}^2 + \hbar v_F J_{ex} (\mathbf{m} \times \mathbf{k})_z, \\ V = \frac{1}{2} \sqrt{4\Delta^2 + (J_{ex} + 2\hbar v_F (\mathbf{m} \times \mathbf{k})_z)^2}.$$

In the above, we have (2×2) energy bands represented by two indexes, *i.e.*, s which has the same meaning as the spin index in Section II, and τ which can be considered as the pseudo-spin index, which refers to the mixing of the top or bottom surface states. By using the same framework as in Section II, we can derive the torque field for each of the energy band as:

$$\mathbf{H}_{s\tau}^{\text{eff}} = s \frac{J_{ex}}{\sqrt{J_{ex}^2 + 4\Delta^2}} \frac{n\hbar v_F}{\mu_0 M_s} (\hat{z} \times \mathbf{k}) \quad (12)$$

for the strong exchange limit ($J_{ex} \gg \hbar v_F k_F$), and

$$\mathbf{H}_{s\tau}^{\text{eff}} = s \frac{J_{ex}}{\sqrt{4\hbar^2 v_F^2 k_F^2 + 4\Delta^2}} \frac{n\hbar v_F}{\mu_0 M_s} (\hat{z} \times \mathbf{k}) \\ + s\tau \frac{\hbar v_F J_{ex} (\mathbf{m} \times \mathbf{k})_z}{2(\hbar^2 v_F^2 k_F^2 + \Delta^2)} \frac{n\hbar v_F}{\mu_0 M_s} (\hat{z} \times \mathbf{k}) \quad (13)$$

for the weak exchange limit ($J_{ex} \ll \hbar v_F k_F$).

Let us first consider the strong exchange limit. If the Fermi energy $E_F = 0$, only the two lower bands contribute to the torque field in Eq. (12), *i.e.*, $s = -1$ and $\tau = \pm 1$. Interestingly, the torque field in Eq. (12) does not depend on the band index τ . Therefore, the total torque field is given by $\mathbf{H}^{\text{eff}} = \sum_{s,\tau} \mathbf{H}_{s\tau}^{\text{eff}} f_{s\tau}$, with $f_{s\tau}$ being the distribution function for each energy bands. The total torque field is given as

$$\mathbf{H}^{\text{eff}} = \eta (\hat{z} \times \mathbf{j}_e^{ss}), \quad (14)$$

where

$$\eta = \frac{\eta_0}{\sqrt{1 + 4(\Delta/J_{ex})^2}}. \quad (15)$$

We see that the direction of the torque field in this case is still the same as in Eq. (6), *i.e.*, in the transverse direction with respect to the applied current. However, the amplitude is now modified by a factor which is a function of the tunneling element Δ as in Eq. 15. Figs. 2 (a), (b) depict the dependence of the torque efficiency $|\mathcal{T}|/j_e^{ss}$ on the tunneling element and the TI thickness, respectively. As expected, for a given surface state current j_e^{ss} ,

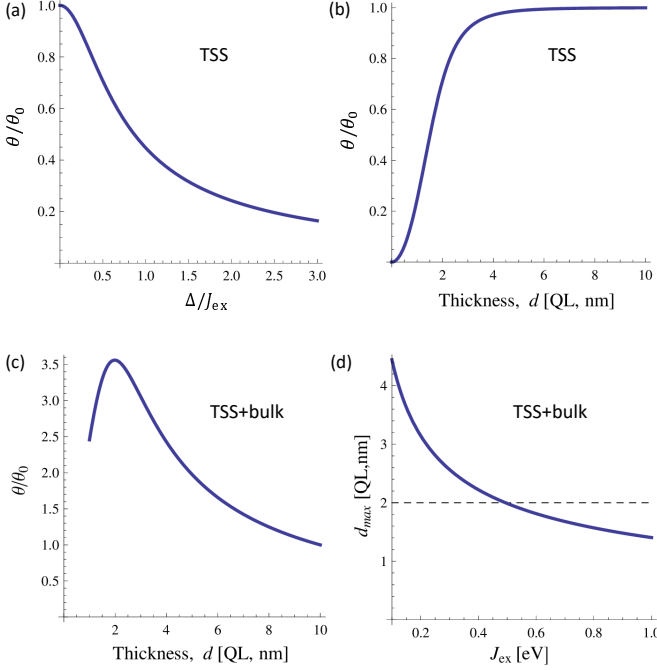


FIG. 2. (Color online) (a), (b) Spin torque efficiency induced by topological surface states (TSS) in an ideal TI in the absence of the bulk channel. (a) Spin torque as a function of the tunneling coupling Δ . (b) Spin torque as a function of thickness d , $J_{\text{ex}} = 0.1$ eV. (c), (d) Spin torque efficiency induced by TSS in the presence of the bulk channel. (c) Torque efficiency as a function of thickness. Comparing to the efficiency in thick film limit (θ_0 normalized to 1), the maximum efficiency is about 3.5 times larger at an optimal thickness $d_{\text{max}} \approx 3$ nm. Parameters used: $J_{\text{ex}} = 0.1$ eV, $G_{\text{TI}}[e^2/h] \sim 19 d$. (d) The value of optimal thickness as a function of exchange coupling for various TI parameter B_1 . The horizontal dashed line represents the effective thickness of the TI surface states (~ 2 nm). The peak of torque efficiency is only observed if the value of d_{max} is above the dashed line. θ_0 is the efficiency at the limit of thick TI film. Parameters used: $B_1 = 0.1$ eV nm² [20]

the torque efficiency is reduced when the Δ increases, a trend which can also be discerned from Eq. (12).

One can check the underlying physics of the torque field reduction by assuming the two surface states have the same helicity. By replacing $-\mathcal{H}_{\text{TI}}$ by \mathcal{H}_{TI} in the bottom right block of Eq. (9), one can find the torque field is $\mathbf{H}^{\text{eff}} = \eta_0 (\hat{z} \times \mathbf{k})$, which is independent of the tunnel coupling Δ . Therefore, we can conclude that it is the coupling between surface states with opposite helicities which reduces the net torque.

B. Thickness optimization

As discussed in previous sections, decreasing TI thickness gives rise to two opposite effects on the spin torque: torque reduction due to the strong surface hybridization,

and torque enhancement due to the weak bulk channel. In this section, we will thus derive the optimal thickness to achieve maximized spin torque.

As the thickness of TI film is reduced, the conductance of the TI film is also diminished [17]. In extremely thin TI films, where the thickness is below 10 nm, the conductance is function of the thickness $G_{\text{TI}}(d) = a_G + b_G d$ [in units of e^2/h]. Meanwhile, in the thick-film limit, the conductance approaches an almost constant value [17]. Experimentally, $b_G \approx 19$ nm⁻¹ for Bi₂Se₃ thin films [17].

The spin torque efficiency, which is the ratio between spin torque and charge current flowing in the TI, *i.e.*, $\theta = \mathcal{T}/j_{\text{TI}}$, is then

$$\theta = \underbrace{\frac{\eta_0}{\sqrt{1 + 4(B_1 \pi^2 / d^2 J_{\text{ex}})^2}}}_{f_1(d) \text{ increases with } d} \underbrace{\left(\frac{G_{\text{TI}}^{\text{ss}}}{a_G + b_G d} \right)}_{f_2(d) \text{ decreases with } d} \quad (16)$$

The above expression is the product of two functions $f_1(d) \cdot f_2(d)$, where f_1 (f_2) increases (decreases) with d . In the limit of large d , $f_1(d) \sim \eta_0$, and $f_2(d)$ is relatively constant with the change in d as the conductance of the TI film is almost unchanged [17], which means that the torque efficiency at large TI thickness would be almost constant. However, in the range of small d , the torque efficiency is more strongly dependent on d . In Fig. 2 (c), the torque efficiency first increases as the thickness is reduced. This is due to the reduction of the bulk contribution to the TI conductance, which enhances the spin-polarized current from the surface state channel. As the thickness is further reduced, the torque efficiency becomes diminished as the hybridization effect becomes the dominant factor. Thus, the torque efficiency reaches a maximum peak at some optimal value of thickness d_{max} .

Now we focus on the maximum efficiency and the corresponding thickness. Basically, these two quantities depend on system's parameters such as B_1 , J_{ex} . For simplicity, we consider the case where $G_{\text{TI}}(d) = b_G d$, for which the maximum efficiency can be analytically found as

$$\theta_{\text{max}} = \frac{\eta_0}{\sqrt{4\pi^2 B_1 / J_{\text{ex}}}} \left(\frac{G_{\text{TI}}^{\text{ss}}}{b_G} \right), \quad (17)$$

corresponding to the optimal thickness of

$$d_{\text{max}} = \sqrt{\frac{2\pi^2 B_1}{J_{\text{ex}}}}. \quad (18)$$

Taking value of the tunneling parameter $B_1 = 0.1$ eV nm², and the exchange coupling $J_{\text{ex}} = 0.1 - 0.5$ eV, the optimal thickness is estimated to be $d_{\text{max}} = 2 - 5$ nm. We note here that, for the maximum torque to be observed, the optimal thickness should not be below the effective thickness of the TI surface states, *i.e.*, $d_{\text{max}} > 2$ nm [16, 17] (see Fig. 2 (d)).

Similarly, we can estimate the optimal thickness in the weak exchange limit, which is given by $d_{\text{max}} =$

$\sqrt{\pi^2 B_1 / \hbar v_F k_F}$. With the Fermi momentum $k_F = 0.07 - 0.14 \text{ \AA}^{-1}$ [17, 27], and the Fermi velocity $v_F \sim 5 \times 10^5 \text{ m/s}$ [20], the optimal thickness is estimated to be in the range of $\sim 1.4 - 2 \text{ nm}$. This range is almost below the effective thickness of the TI surface state, and thus the optimal spin torque may not be observed in the weak exchange regime.

IV. CONCLUSION

In this paper, we have analytically derived the spin-orbit torque induced by a thin TI film. First, we showed that in thin TI films, the spin torque is reduced due to the surface hybridization effect. This decrease is a consequence of the opposite helicities of the surface states on the two surfaces. On the other hand, lowering the thickness of the TI film may have a positive effect on the spin torque by reducing the bulk channel contribution to the total conductance. This increases the proportion of current flowing through the surface states, which constitutes

the source of the current-induced torque on the magnetic layer. Due to these opposing trends, there thus exists an optimal TI thickness at which the torque efficiency is maximized. Based on typical experimental parameter values, we found that the torque efficiency at the optimal thickness to be several times larger than the torque values at the thick TI-layer limit. Our prediction for the optimal thickness is within the practical range which can be verified experimentally.

ACKNOWLEDGMENTS

We acknowledge the financial support of MOE Tier II grant MOE2013-T2-2-125 (NUS Grant No. R-263-000-B10-112), and the National Research Foundation of Singapore under the CRP Programs Next Generation Spin Torque Memories: From Fundamental Physics to Applications NRF-CRP12-2013-01 and Non-Volatile Magnetic Logic and Memory Integrated Circuit Devices NRF-CRP9-2011-01.

-
- [1] S. G. Tan, M. B. A. Jalil, X.-J. Liu, and T. Fujita, [arXiv:0705.3502](#) (2007); S. G. Tan, M. B. A. Jalil, T. Fujita, and X.-J. Liu, *Ann. Phys. (NY)* **326**, 207 (2011).
 - [2] A. Manchon and S. Zhang, *Phys. Rev. B* **78**, 212405 (2008).
 - [3] A. Matos-Abiague and R. L. Rodríguez-Suárez, *Phys. Rev. B* **80**, 094424 (2009).
 - [4] I. M. Miron, G. Gaudin, S. Auffret, B. Rodmacq, A. Schuhl, S. Pizzini, J. Vogel, and P. Gambardella, *Nat. Mater.* **9**, 230 (2010).
 - [5] H. Li, H. Gao, L. P. Zárbo, K. Výborný, X. Wang, I. Garate, F. Doğan, A. Čejchan, J. Sinova, T. Jungwirth, and A. Manchon, *Phys. Rev. B* **91**, 134402 (2015).
 - [6] P. M. Haney, H.-W. Lee, K.-J. Lee, A. Manchon, and M. D. Stiles, *Phys. Rev. B* **87**, 174411 (2013).
 - [7] H. Kurebayashi, J. Sinova, D. Fang, A. Irvine, T. Skinner, J. Wunderlich, V. Novak, R. Campion, B. Gallagher, and E. Vohst, *Nat. Nanotechnol.* **9**, 211 (2014).
 - [8] I. Miron, G. Gaudin, S. Auffret, B. Rodmacq, A. Schuhl, S. Pizzini, J. Vogel, and P. Gambardella, *Nat. Mater.* **9**, 230 (2010).
 - [9] A. Mellnik, J. Lee, A. Richardella, J. Grab, P. Mintun, M. Fischer, A. Vaezi, A. Manchon, E.-A. Kim, and N. Samarth, *Nature* **511**, 449 (2014).
 - [10] Y. Wang, P. Deorani, K. Banerjee, N. Koirala, M. Brahlek, S. Oh, and H. Yang, *Phys. Rev. Lett.* **114**, 257202 (2015).
 - [11] Y. Fan, P. Upadhyaya, X. Kou, M. Lang, S. Takei, Z. Wang, J. Tang, L. He, L.-T. Chang, and M. Montazeri, *Nat. Mater.* **13**, 699 (2014).
 - [12] V. M. Edelstein, *Solid State Communications* **73**, 233 (1990).
 - [13] S. Murakami, N. Nagaosa, and S.-C. Zhang, *Science* **301**, 1348 (2003).
 - [14] T. Fujita, M. Jalil, and S. Tan, *New J. Phys.* **12**, 013016 (2010).
 - [15] K. Kuroda, M. Arita, K. Miyamoto, M. Ye, J. Jiang, A. Kimura, E. E. Krasovskii, E. V. Chulkov, H. Iwasawa, T. Okuda, K. Shimada, Y. Ueda, H. Namatame, and M. Taniguchi, *Phys. Rev. Lett.* **105**, 076802 (2010).
 - [16] J. Linder, T. Yokoyama, and A. Sudbø, *Phys. Rev. B* **80**, 205401 (2009).
 - [17] N. Bansal, Y. S. Kim, M. Brahlek, E. Edrey, and S. Oh, *Phys. Rev. Lett.* **109**, 116804 (2012).
 - [18] G. Zhang, H. Qin, J. Teng, J. Guo, Q. Guo, X. Dai, Z. Fang, and K. Wu, *Appl. Phys. Lett.* **95**, 053114 (2009).
 - [19] H. Peng, K. Lai, D. Kong, S. Meister, Y. Chen, X.-L. Qi, S.-C. Zhang, Z.-X. Shen, and Y. Cui, *Nat. Mater.* **9**, 225 (2010).
 - [20] Y. Zhang, K. He, C.-Z. Chang, C.-L. Song, L.-L. Wang, X. Chen, J.-F. Jia, Z. Fang, X. Dai, W.-Y. Shan, S.-Q. Shen, Q. Niu, X.-L. Qi, S.-C. Zhang, X.-C. Ma, and Q.-K. Xue, *Nat. Phys.* **6**, 584 (2010).
 - [21] J. Linder, T. Yokoyama, and A. Sudbø, *Phys. Rev. B* **80**, 205401 (2009).
 - [22] H.-Z. Lu, W.-Y. Shan, W. Yao, Q. Niu, and S.-Q. Shen, *Phys. Rev. B* **81**, 115407 (2010).
 - [23] C.-X. Liu, H. Zhang, B. Yan, X.-L. Qi, T. Frauenheim, X. Dai, Z. Fang, and S.-C. Zhang, *Phys. Rev. B* **81**, 041307 (2010).
 - [24] A. Zyuzin, M. Hook, and A. Burkov, *Phys. Rev. B* **83**, 245428 (2011).
 - [25] S. S. Pershoguba and V. M. Yakovenko, *Phys. Rev. B* **86**, 165404 (2012).
 - [26] M. B. A. Jalil, personal communication (2016).
 - [27] K. Hoefer, C. Becker, D. Rata, J. Swanson, P. Thalmeier, and L. H. Tjeng, *PNAS* **111**, 14979 (2014).